

## Theoretical study of the large linear dichroism of herapathite

Lei Liang,<sup>1</sup> Paul Rulis,<sup>1</sup> Bart Kahr,<sup>2</sup> and W. Y. Ching<sup>1</sup>

<sup>1</sup>*Department of Physics, University of Missouri-Kansas City, Kansas City, Missouri 64110, USA*

<sup>2</sup>*Department of Chemistry, New York University, New York, New York 10003, USA*

(Received 23 July 2009; revised manuscript received 30 November 2009; published 30 December 2009)

The remarkable linear dichroism of herapathite (HPT), the active component of polaroid, resisted explanation for more than 150 years because the crystal structure was not solved until very recently. The crystal structure with a formula unit of  $(C_{20}H_{24}N_2O_2H_2)_4 \cdot C_2H_4O_2 \cdot 3SO_4 \cdot 2I_3 \cdot 6H_2O$  in an orthorhombic cell has a slight disorder related to the positions of the six water molecules and the acetic-acid molecule. The electronic and optical properties of this complex crystal are here calculated on the basis of the newly described x-ray structure using a density-functional theory based method with local-orbital basis. The theoretical optical spectrum of HPT shows giant optical anisotropy as observed experimentally with an anisotropy factor on the order of 385 that can be ascribed to transitions between molecular levels of the  $2I_3^-$  chains that are oriented along the crystalline  $b$  axis. It is shown that the key to achieve large anisotropy is to align the iodine ions in a quasi-one-dimensional chain via confinement in a clathrate channel formed by the quinine molecules. The solvent molecules in the crystal have a minimal effect. The implications of this work on biologically relevant systems are discussed.

DOI: [10.1103/PhysRevB.80.235132](https://doi.org/10.1103/PhysRevB.80.235132)

PACS number(s): 78.40.Me, 71.15.Ap, 71.20.Rv, 78.20.-e

### I. INTRODUCTION

The herapathite (HPT) crystal was accidentally discovered in 1852.<sup>1</sup> It was immediately realized that this iodine containing quinine crystal had a uniquely strong anisotropy in the optical spectrum.<sup>1-3</sup> During the 150 years since its discovery, scientists have been intrigued by the strong linear dichroism and have found numerous applications for its polarizing properties.<sup>4</sup> The formula of the HPT unit cell was established soon after its discovery as  $4QH_2^{2+} \cdot 3SO_4^{2-} \cdot 2I_3^- \cdot 6H_2O$ , where  $Q=C_{20}H_{24}N_2O_2$  (quinine) (Ref. 5) but its x-ray structure was slow in coming due to the complex composition of HPT and because the crystals were extremely fragile and often twinned. As a result, the electronic structure of this crystal with homoatomic trihalide anions in an organic matrix was not defined and a proper explanation of its giant optical anisotropy could not be articulated.

Recently, the structure of crystalline HPT was fully resolved using x-ray diffraction techniques.<sup>6</sup> It has a formula unit of  $4QH_2^{2+} \cdot C_2H_4O_2 \cdot 3SO_4^{2-} \cdot 2I_3^- \cdot 6H_2O$  in an orthorhombic cell (space group  $P22_12_1$ , No. 18,  $Z=4$ ). The crystal contains an acetic-acid molecule  $C_2H_4O_2$  in addition to the components identified by Jörgensen.<sup>5</sup> Six water molecules are distributed over eight possible sites and the acetic-acid molecule is distributed over two possible sites. The full unit cell contains a total of 988 atoms (2864 electrons excluding core electrons) (Fig. 1). The triiodide chains run in a clathrate channel formed by quinine molecules. The six I atoms are crystallographically nonequivalent with intratriiodide I-I separations of 2.888, 3.012, 2.937, and 2.968 Å and intertriiodide I $\cdots$ I separations of 3.743 and 3.810 Å which are similar to those in other triiodide systems.<sup>7</sup> Each of the  $I_3^-$  anions is almost linear but they are not parallel to the crystallographic  $b$  axis. Instead, they zigzag by  $\pm 12^\circ$  toward the  $c$  axis.

In this paper, we report a detailed theoretical calculation on the electronic structure and the linear optical properties of

the HPT crystal based on this recently determined structure. The origin of the giant anisotropy observed in this crystal is fully explained by a critical analysis of the molecular orbitals of the  $I_3^-$  ions in the organic matrix and the implication of the results on complex biomolecular systems are discussed.

### II. METHOD AND RESULTS OF CALCULATION

The *ab initio* calculation of the electronic structure of a complex crystal such as HPT with all the solvent molecules and counterions is a great challenge in computational chemistry and physics. We used the orthogonalized linear combination of atomic orbitals (OLCAO) method<sup>8</sup> to calculate the electronic-structure and linear optical properties of HPT. OLCAO is a density-functional theory<sup>9</sup> based method with local approximations to the exchange-correlation potential. The use of atomic orbitals in the basis expansion makes the OLCAO method highly efficient for complex multicomponent systems with large cells and is applicable to both inorganic<sup>10</sup> and organic crystals.<sup>11</sup> A large basis set is used for the HPT calculation consisting of I (Kr core plus  $5s, 5p, 6s, 6p, 5d$ ), S (Ne core plus  $3s, 3p, 4s, 4p, 3d$ ), O (He core plus  $2s, 2p, 3s, 3p$ ), H ( $1s, 2s, 2p$ ), N (He core plus  $2s, 2p, 3s, 3p$ ), and C (He core plus  $2s, 2p, 3s, 3p$ ) atomic orbitals in the self-consistent field iterations. The core states are later eliminated from the final secular equation using the orthogonalization technique.<sup>8</sup> To increase the accuracy for the optical calculation, the basis functions are further expanded to include additional higher unoccupied orbitals for each atom such that the final secular equation has the size of  $14\,191 \times 14\,191$  after orthogonalization. All energy eigenvalues and eigenvectors are obtained at the  $\Gamma$  (0,0,0) point of the Brillouin zone (BZ). Due to the very large cell size, the corresponding BZ is very small and the use of one  $k$  point in the calculation is fully justified.

To account for the partial occupation of sites in HPT associated with the disorder, we carried out OLCAO calcula-

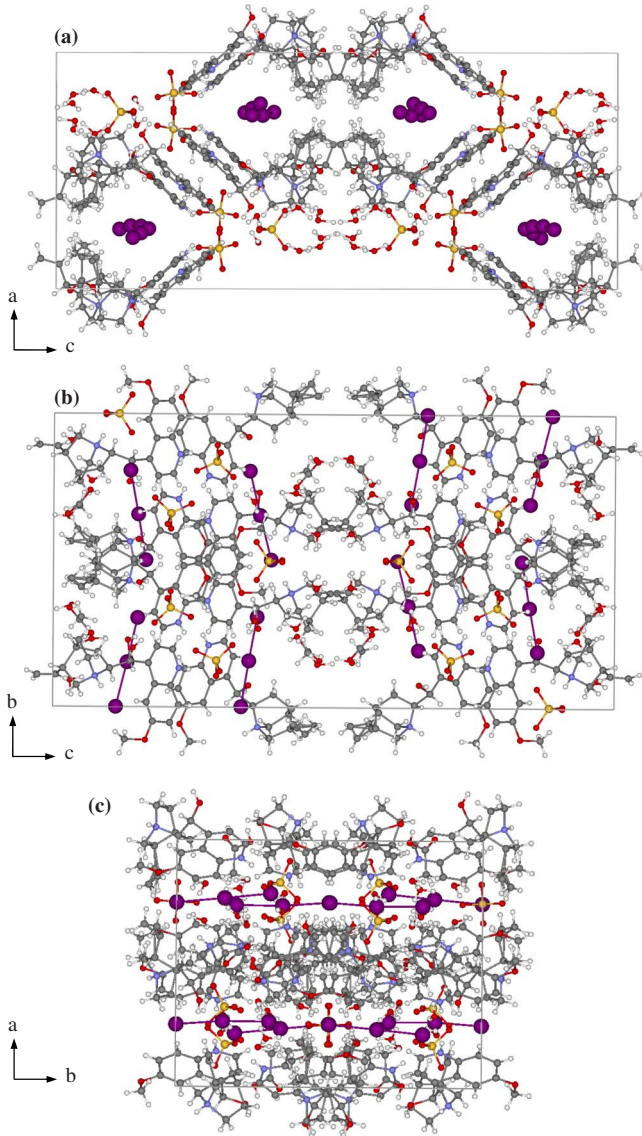


FIG. 1. (Color online) Crystal structure of HPT viewed in the (a) [010], (b) [100], and (c) [001] directions to show the position and orientation of  $I_3^-$  chains within the organic matrix. I (large violet), S (yellow), O (red), C (gray), and H (white).

tions on six HPT models with different distributions of acetic-acid and water molecules over the available sites. The results are listed in Table I and they are almost the same indicating that the slight disorder does not meaningfully affect the electronic structure of the crystal. For the purpose of discussion, we present the result from model 6. Figure 2(a) shows the calculated total density of states (DOS) of model 6 with a slight 0.02 eV Gaussian broadening of the molecular-orbital (MO) levels. Also shown [Fig. 2(b)] are the partial DOS (PDOS) of group components: triiodide, quinine, sulfate, acetic acid, and water. The calculated band gaps, or equivalently, the separations of highest occupied molecular orbital (HOMO) and lowest unoccupied molecular orbital (LUMO) range from 0.40 to 0.78 eV depending on the model (see Table I). The HOMO (set at 0.0 eV) comes from  $I_3^-$  states and the LUMO from the quinine states. Transitions from occupied iodine states account for the strong optical absorptions in the visible region (400–700 nm) and will be detailed later. It can be noted that within the range of  $-1.2$  to  $+2.0$  eV, the only states involved are those of  $I_3^-$  and quinine. These iodine states do not change with different models whereas the quinine states do shift slightly due to subtle disorder-induced differences. The solvent molecules do not contribute to the optical transitions in HPT and the quinine states affect it only slightly. We have also calculated the effective charges  $Q^*$  on each ion in HPT using the minimal basis Mulliken scheme.<sup>12</sup> For the six crystallographically nonequivalent  $I_3^-$  ions, the charges are  $-0.322$ ,  $-0.071$ ,  $-0.487$ ,  $-0.382$ ,  $-0.060$ , and  $-0.431$  electron for I1, I2, I3, I4, I5, and I6, respectively, so that the ionic description of  $I_3^-$  for the triiodide chain (I1-I2-I3 or I4-I5-I6) is reasonably accurate. The central I atoms carry less charge which is typical for 3-center 4-electron ( $3c, 4e$ ) bonding in  $I_3^-$ .<sup>13</sup> However, as will be shown later, the inter- $I_3^-$  interactions in the chain are not negligible so it is appropriate to view I atoms in HPT as an infinite one-dimensional chain of  $I_3^-$  units running along the crystallographic  $b$  axis. The Mulliken effective charges for six iodine ions in the other models are listed in Table I.

To further obtain the insights on the charge transfer in the HPT crystal, we have calculated the charge-density distribution from the OLCAO calculation using a dense mesh of

TABLE I. Summary of main results on the six models for HPT calculations.

	Model 1	Model 2	Model 3	Model 4	Model 5	Model 6
HOMO-LUMO gap (eV)	0.40	0.61	0.58	0.78	0.063	0.73
Peak location (eV)						
A	1.77	1.77	1.78	1.77	1.76	1.76
B	1.54	1.56	1.56	1.57	1.56	1.56
Anisotropy factor	360	416	423	421	375	316
	$Q^*$ for iodine atoms (electrons)					
I1	7.327	7.322	7.329	7.322	7.323	7.322
I2	7.080	7.084	7.070	7.070	7.082	7.071
I3	7.471	7.480	7.478	7.488	7.481	7.487
I4	7.383	7.409	7.383	7.384	7.406	7.382
I5	7.057	7.055	7.062	7.061	7.056	7.060
I6	7.432	7.408	7.430	7.430	7.412	7.431

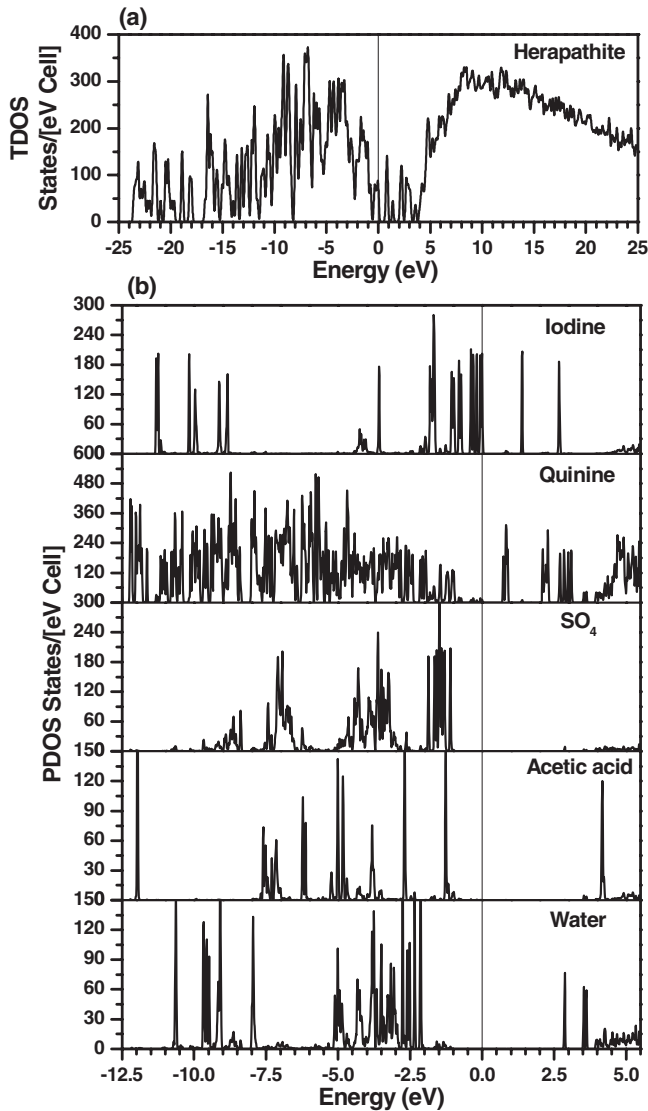


FIG. 2. (a) Total DOS of HPT. (b) Partial DOS of different groups: triiodide, quinine, sulfate, acetic acid, and water.

200 × 300 × 600. Figure 3 shows the electron-density difference map between the calculated charge density and the neutral atom charge density at the same locations on the crystal-line  $bc$  plane which approximately contains the iodine chain. It can be seen that within this particular plane, the atoms that

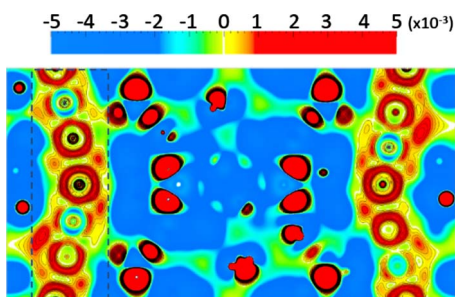


FIG. 3. (Color online) Calculated charge-density deviation of HPT in the  $bc$  plane (see text for details). The dashed line identifies a portion analyzed in Fig. 5(c).

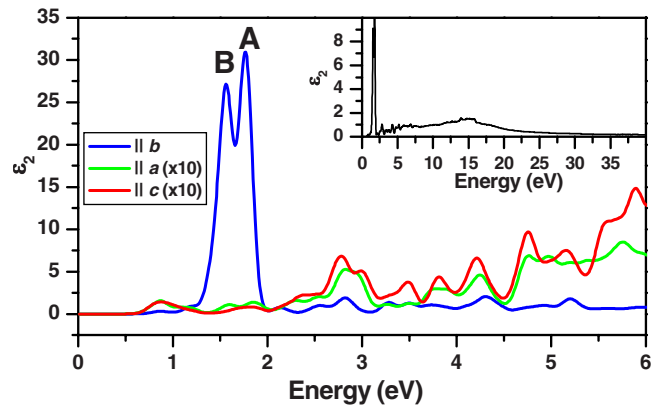


FIG. 4. (Color online) Calculated  $\epsilon_2(\hbar\omega)$  of HPT for component  $\parallel$  to  $b$  axis (blue) and  $\perp$  to  $b$  axis (red, green). Inset shows the averaged spectrum up to 40 eV.

gain charges (more negative) are those from the iodine and some O or C atoms in the solvent molecules. Most parts of the crystal which contain quinine and other solvent molecules are losing some charges (more positive). This could indicate the presence of some longer-range interactions between the  $I_3^-$  ions and the organic matrix that contains them.

The optical transitions in the HPT crystal are calculated as the imaginary part of the dielectric function  $\epsilon_2(\hbar\omega)$  within the random-phase approximation<sup>14</sup> with an extended basis set,

$$\epsilon_2(\hbar\omega) = \frac{e^2}{\pi m \omega^2} \int_{\text{BZ}} dk^3 \sum_{n,l} |\langle \psi_n(\vec{k}, \vec{r}) | -i\hbar \vec{\nabla} | \psi_l(\vec{k}, \vec{r}) \rangle|^2 \delta[E_n(\vec{k}) - E_l(\vec{k}) - \hbar\omega].$$

Here the BZ integration is just for the  $\Gamma$  point and  $n$  and  $l$  represent the unoccupied and occupied states of HPT, respectively. Such calculations have been successfully applied to many complex crystals<sup>15,16</sup> including carbon nanotubes.<sup>17,18</sup> Although there are more advanced theories in recent years for describing optical excitations in molecules and crystals such as time-dependent density-functional theory or the inclusion of excitonic effects based on many-body theory, they cannot yet be applied to large complex crystals such as herapathite.

Figure 4 shows the calculated  $\epsilon_2(\hbar\omega)$  up to 6 eV for the three components parallel to the  $a$ ,  $b$ , and  $c$  axes of the crystal. The inset shows the averaged spectrum up to 40 eV in the far ultraviolet region. There is a huge absorption manifest as a doubled peak (marked as A and B) at 1.76 and 1.56 eV in the direction parallel to the  $b$  axis whereas absorptions in the perpendicular directions are negligible. We define the optical anisotropy factor (OAF) or linear dichroism as the ratio of the amplitude for absorption in the  $b$  direction to the average of amplitudes at the same energy in  $a$  and  $c$  directions for peak A. Table I shows that the OAF ranges from 316 to 423 for the six models with the average value of 385. While anisotropic absorption in HPT was described by its discover,<sup>1</sup> the *ab initio* calculation provides a basis for this property in terms of electronic structure. Land and West in 1946 published HPT spectra<sup>4</sup> showing the absorption maxi-



mum to be around  $\sim 2.2$  eV but no detailed spectral features are available. The difference in experimental and theoretical energies can be explained by the well-known fact that local-density approximation calculations generally underestimate the band gap of insulators by roughly 20–30%. There are additional weak structures above 2 eV and a broad peak at 15 eV. They originate from transitions in the quinine, sulfate, and solvent molecules. These optical absorptions and their origin may be of importance in other complex crystals or biological systems; we will not discuss them in the present paper.

### III. DISCUSSIONS

What then is the origin of this giant optical anisotropy in HPT? The proper interpretation can be complicated by three factors. First, there are considerable interactions between the two  $I_3^-$  ions so a simple interpretation based on MOs of  $I_3^-$  with  $C_{\infty h}$  symmetry is not adequate since the symmetry is broken. Second, the two  $I_3^-$  ions are not strictly linear and their axial direction deviates from the  $z$  direction ( $b$  axis) by  $\pm 12^\circ$ . Third, the  $I_3^-$  ions do interact weakly with the quinine molecules with further mixing from non-I components. We have identified all 22 MOs (44 electrons) and have verified the splitting as being due to interaction between the two  $I_3^-$  ions by separately calculating the MOs of the two  $I_3^-$  ions individually and together, without the quinine and solvent molecules. Six MOs from the I  $5s$  electrons are located below  $-8.5$  eV [Fig. 5(a)]. The remaining 32  $5p$  electrons form 16 MO orbitals that are above  $-4.5$  eV. 12 of these MOs are of approximate  $\pi$  symmetry (with  $p_x$ - and  $p_y$ -orbital symmetry). The remaining four MOs are part of the  $(3c-4e)$  bond in each of the  $I_3^-$  ions. They have approximate  $\sigma$  character dominated by the  $p_z$  orbital. To delineate the geometric effect of the molecular arrangement in HPT, the orbital-resolved PDOS of these 16 MOs in the  $-4.5$ – $1.5$  eV range are shown in Fig. 5(b). The strong transitions, A and B, from the two  $\sigma$ -like states (at  $-0.39$  and  $-0.18$  eV) with transition energies of 1.76 and 1.56 eV are marked. These two states, which give rise to the double peak in Fig. 4, are due to the splitting of the  $\sigma$ -like MO when the two  $I_3^-$  ions interact and these are dominated by the  $5p_z$  orbital with some mixing from  $5p_y$ . This mixing is due to the fact that the axial directions of the two  $I_3^-$  ions are not the same as the Cartesian  $z$  direction in the calculation [see Fig. 1(b)]. The mixing allows for maximum overlap in the axial direction of  $I_3^-$  between the initial and final  $\sigma$ -like states in the optical transition giving rise to the large linear dichroism. Interestingly, there is about 7% participation from the  $5d_{3z^2-r^2}$  orbital of I to the  $\sigma$  level due to its favorable overlap in the  $z$  direction. By further resolving the PDOS into each individual I atom, we find the orbital mixing of the central I atoms (I2 and I4) to be different from the end I atoms (I1, I3, I4, and I6) where extra charge accumulates. The state that gives rise to the peak A at  $-0.39$  eV is dominated by the  $p_z$  orbitals of I1 and I4 whereas the state that gives rise to the peak B at  $-0.18$  eV has substantial contributions from the other end atoms I3 and I6. This underscores the asymmetric nature of the two  $I_3^-$  ions and their interactions that result in the double peak. On the other hand,

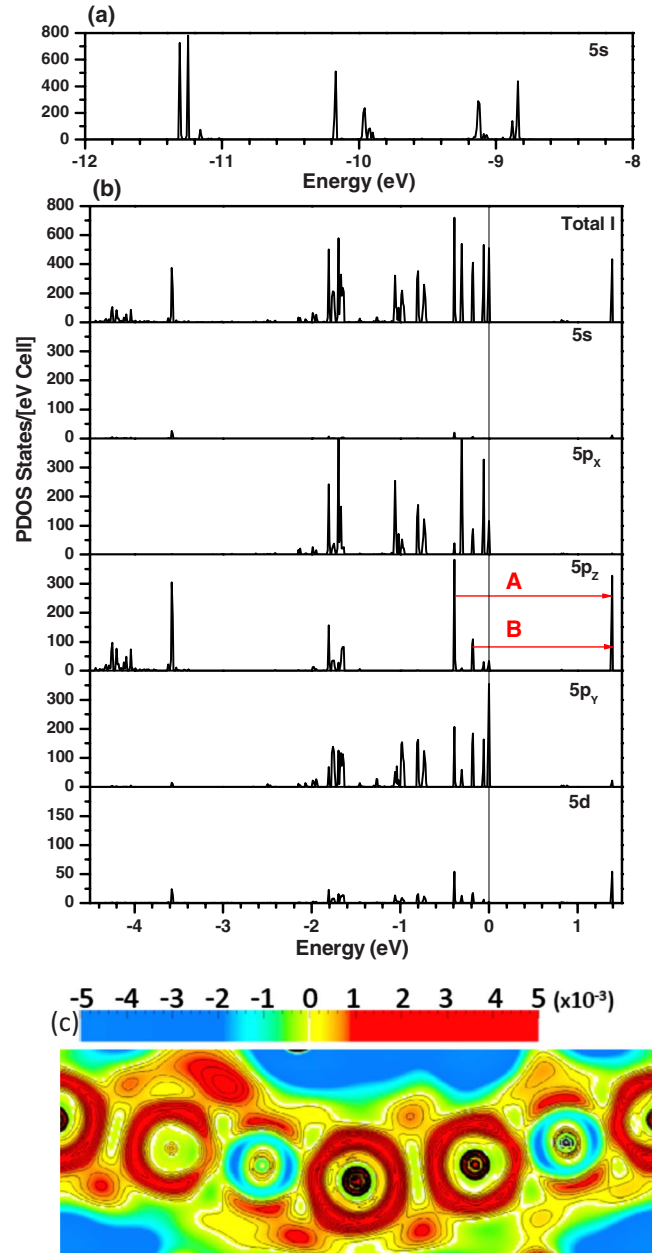


FIG. 5. (Color online) (a) Molecular-orbital diagram showing transitions for the strong doubled absorption peaks (A and B); (b) orbital-resolved PDOS for I states between  $-1.5$  and  $1.5$  eV. (c) Distribution of real-space charge difference from neutral atoms on the six I ion chain in the crystalline  $bc$  plane showing different charge transfer on the six I atoms (I1–I6) and the interaction between two  $I_3^-$  ions in the unit of electrons/cell volume.

the two  $\sigma$ -like states between  $-4.4$  and  $-3.5$  eV are exclusively from the  $p_z$  orbital of the central I and do not participate in any appreciable optical transition. Also, some of the MOs (those near  $-4.3$  and  $-1.7$  eV) are somewhat delocalized as can be seen from the much broadened peaks with noticeable interactions with the quinine. Figure 5(c) shows the charge-density deviation of the six I atoms in the  $bc$  plane in HPT extracted from Fig. 3.

#### IV. SUMMARY AND CONCLUSIONS

In this paper, we have elucidated the origin of the giant optical anisotropy with an optical anisotropy factor on the order of 385 in the linearly dichroic herapathite crystal by means of *ab initio* electronic-structure calculation. The clathrate channel formed by quinine molecules contains and aligns the triiodide chain. This key arrangement allows for I  $5p_z$ -orbital alignment and subsequently strong transitions from the  $\sigma$ -like to  $\sigma^*$ -like molecular-orbital state of two  $I_3^-$  with transition energies around 1.6–1.8 eV consistent with experimental observations. The interactions between the triiodides in the quasi-one-dimensional triiodide chain play a key role in the positions of I MO levels resulting in the predicted double-peak feature. The solvent molecules and their disorder in the crystal have no large effect other than on the size of the band gap since the LUMO state is determined by the states from the quinine molecules. There are some small interactions between I and H from quinine.

It is known that HPT and other similar dichroic systems have great application in polarization-dependent devices but we anticipate that fundamental understanding of the electronic and optical properties of HPT can facilitate the development of new applications through the controlled modification of the crystal structure. In biologically relevant systems

such as DNA and proteins, large linear and circular dichroism is common.<sup>19</sup> It is extremely difficult to obtain optical-absorption spectra for complex biomolecular systems by experimental means especially for transitions to higher photon energies. *Ab initio* calculation of optical spectra can provide such data which could potentially lead to quantitative evaluation of van der Waals forces<sup>20</sup> through the electrodynamic theory of Lifshitz<sup>21</sup> as recently demonstrated in the carbon nanotube systems.<sup>17,18</sup> We believe that accurate optical spectral calculation for complex crystals and molecules can play a significant role in the understanding the long-range interactions at nanoscale.<sup>22</sup>

#### ACKNOWLEDGMENTS

This work is supported by the U.S. Department of Energy, Office of Basic Energy Sciences, Division of Materials Science and Engineering under the Grant No. DE-FG02-84DR45170. This research used the resources of NERSC supported by the Office of Science of DOE under the Contract No. DE-AC03-76SF00098. B.K. is supported by NSF under Grant No. CHE-0349882. Lei Liang is supported by the funding from University of Missouri Research Board. We thank many colleagues who have made constructive comments on this manuscript.

<sup>1</sup>W. B. Herapath, *Philos. Mag.* **3**, 161 (1852).

<sup>2</sup>W. B. Herapath, *Philos. Mag.* **6**, 346 (1853).

<sup>3</sup>G. G. Stokes, *Philos. Mag.* **6**, 393 (1853).

<sup>4</sup>E. H. Land and C. D. West, in *Colloid Chemistry*, edited by J. Alexander (Van Nostrand, New York, 1946), Vol. 6, p. 160.

<sup>5</sup>S. M. Jørgensen, *J. Prakt. Chem.* **14**, 215 (1877).

<sup>6</sup>B. Kahr, J. Freudenthal, S. Phillips, and W. Kaminsky, *Science* **324**, 1407 (2009).

<sup>7</sup>P. H. Svensson and L. Kloo, *Chem. Rev. (Washington, D.C.)* **103**, 1649 (2003).

<sup>8</sup>W. Y. Ching, *J. Am. Ceram. Soc.* **73**, 3135 (1990).

<sup>9</sup>W. Y. Ching, Paul Rulis, Lizhi Ouyang, and Anil Misra, *Appl. Phys. Lett.* **94**, 051907 (2009).

<sup>10</sup>L. Ouyang, L. Randaccio, P. Rulis, E. Z. Kurmaev, A. Moewes, and W. Y. Ching, *J. Mol. Struct.: THEOCHEM* **622**, 221 (2003).

<sup>11</sup>P. Hohenberg and W. Kohn, *Phys. Rev.* **136**, B864 (1964); W. Kohn and L. J. Sham, *ibid.* **140**, A1133 (1965).

<sup>12</sup>R. S. Mulliken, *J. Chem. Phys.* **23**, 1841 (1955).

<sup>13</sup>G. A. Landrum, N. Goldberg, and R. Hoffmann, *J. Chem. Soc. Dalton Trans.* 1997 3605.

<sup>14</sup>H. Ehrenreich and M. H. Cohen, *Phys. Rev.* **115**, 786 (1959).

<sup>15</sup>S.-D. Mo, L. Ouyang, W. Y. Ching, I. Tanaka, Y. Koyama, and R. Riedel, *Phys. Rev. Lett.* **83**, 5046 (1999).

<sup>16</sup>W. Y. Ching and P. Rulis, *Phys. Rev. B* **77**, 035125 (2008).

<sup>17</sup>R. F. Rajter, R. Podgornik, V. A. Parsegian, R. H. French, and W. Y. Ching, *Phys. Rev. B* **76**, 045417 (2007).

<sup>18</sup>A. Siber, R. F. Rajter, R. H. French, W. Y. Ching, V. A. Parsegian, and R. Podgornik, *Phys. Rev. B* **80**, 165414 (2009).

<sup>19</sup>A. Rodger and B. Nordén, *Circular Dichroism and Linear Dichroism* (Oxford University Press, Oxford, 1997).

<sup>20</sup>V. A. Parsegian, *Van der Waals Forces* (Cambridge University Press, Cambridge, England, 2005).

<sup>21</sup>E. M. Lifshitz, *Sov. Phys. JETP* **2**, 73 (1956).

<sup>22</sup>R. H. French, V. A. Parsegian *et al.*, *Rev. Mod. Phys.* (to be published).